Molecular Vision 2013; 19:2596-2605 <http://www.molvis.org/molvis/v19/2596>
Received 19 July 2013 | Accepted 23 December 2013 | Published 27 December 2013

A novel rat contact lens model for *Fusarium* keratitis

Mohamed Abou Shousha,[1,2] Andrea Rachelle C. Santos,[1] Rafael A. Oechsler,[1,3] Alfonso Iovieno,[1,4] Jorge Maestre-Mesa,[1] Marco Ruggeri,[1] Jose J. Echegaray,[1] Sander R. Dubovy,[1] Victor L. Perez,[1] Darlene Miller,[1] Eduardo C. Alfonso,[1] M. Livia Bajenaru[1]

(The first two authors contributed equally to this work)

[1]Bascom Palmer Eye Institute, University of Miami Miller School of Medicine, Miami; [2]Department of Ophthalmology, Saint Louis University School of Medicine, St. Louis, MO; [3]Department of Ophthalmology, Federal University of Sao Paulo, Sao Paulo, Brazil; [4]Department of Ophthalmology, University Campus Bio-medico, Rome, Italy

Purpose: The aim of this study was to develop and characterize a new contact lens–associated fungal keratitis rat model and to assess the ability of non-invasive spectral-domain optical coherence tomography (SD-OCT) to detect pathological changes in vivo in fungal keratitis.

Methods: We used SD-OCT to image and measure the cornea of Sprague Dawley rats. *Fusarium* infection was initiated in the rat eye by fitting *Fusarium solani*–soaked contact lenses on the experimental eye, while the control animals received contact lenses soaked in sterile saline. The fungal infection was monitored with periodic slit-lamp examination and in vivo SD-OCT imaging of the rat eye, and confirmed by histology, counting of viable fungi in the infected rat cornea, and PCR with specific primers for *Fusarium sp.*

Results: We imaged and measured the rat cornea with SD-OCT. Custom-made contact lenses were developed based on the OCT measurements. Incubation of contact lenses in a *F. solani* suspension resulted in biofilm formation. We induced contact lens–associated *Fusarium* keratitis by fitting the rat eyes for 4 h with the *Fusarium*-contaminated contact lenses. The SD-OCT images of the cornea correlated well with the slit-lamp and histopathological results and clearly defined clinical signs of infection, namely, increased corneal thickening, loss of epithelial continuity, hyper-reflective areas representing infiltrates, and endothelial plaques characteristic of fungal infection. Moreover, in three cases, SD-OCT detected the infection without any clear findings on slit-lamp examination. Infection was confirmed with histological fungal staining, PCR, and microbiological culture positivity.

Conclusions: We developed a highly reproducible rat contact lens model and successfully induced contact lens–associated *Fusarium* keratitis in this model. The clinical presentation of contact lens–associated *Fusarium* keratitis in the rat model is similar to the human condition. SD-OCT is a valuable tool that non-invasively revealed characteristic signs of the fungal infection and could provide sensitive, objective monitoring in fungal keratitis.

Corneal blindness is a major public health problem, and infectious keratitis is a predominant cause [1]. One of the most important risk factors for infectious keratitis is extended and overnight contact lens wear [2]. Five to twenty percent of all infectious keratitis cases are of fungal etiology [3, 4]. Fungal keratitis is a sight-threatening infection of the cornea that carries worse prognosis than other types of microbial keratitis. Delayed diagnosis and relative resistance to treatment typical for fungal keratitis make the fungal infection 5–6 times more likely to affect the integrity of the globe and extend to the anterior chamber of the eye than bacterial keratitis [5]. One third of cases of fungal keratitis are related to contact lens wear [6]. Although the incidence of developing infective keratitis from contact lens wear is low, the high prevalence and chronicity of contact lens wear make it a serious public health problem. In 2005, an outbreak of contact lens–related *Fusarium* keratitis drew the attention of the world and emphasized the significance of this serious infection. Ninety-four percent of the affected individuals were soft contact lens wearers, and one third of the cases required corneal transplantation [7-12]. Owing to these facts, we were interested in closely studying contact lens–related fungal keratitis, in particular that caused by *Fusarium*, a fungus that is the most common causative organism for the disease [10].

Optical coherence tomography (OCT) is a relatively new non-contact imaging technology that provides cross-sectional images (tomography) of internal structures in biologic tissues. Spectral domain optical coherence tomography (SD-OCT), a newer implementation of OCT, has shorter acquisition time and higher axial resolution than the conventional time domain optical coherence tomography (TD-OCT) and thus provides denser cross-sectional sampling of the tissue. The introduction of SD-OCT technology, which can study the eye in resolutions down to a few microns, carries significant hope

Correspondence to: M. Livia Bajenaru, Bascom Palmer Eye Institute, University of Miami Miller School of Medicine, PO Box 016880, Miami, FL 33101; Phone: (305) 547-3714; FAX: (305) 547-3658; email: lbajenaru@med.miami.edu

to improve our diagnostic capabilities. SD-OCT has quickly become among the standard of care of retinal diseases such as macular degeneration [13] and glaucoma [14]. Only recently, OCT has been used for imaging the anterior segment and the cornea in anterior chamber biometry [15], anterior segment tumors [16], and corneal refractive surgery [17]. Several valuable studies of infectious keratitis by OCT have emerged; however, these studies used TD-OCT with resolutions of 18 microns, significantly lower than the 3 micron resolution of the new generations of SD-OCT [18,19].

In an effort to study risk factors and pathogenicity for microbial ocular infections and to improve diagnosis with molecular and imaging techniques, we developed a highly reproducible rat contact lens model with the help of sophisticated OCT techniques. Our animal model puts us in a good position to evaluate the molecular, cellular, and radiographic features of the disease formation. Given the importance and morbidity of *Fusarium* keratitis, we decided to use the newly developed contact lens animal model to induce and better characterize this infection. We used classical diagnostic methods such as fungal culture, histology, and slit-lamp examination to characterize this infection. Additionally, we evaluated new approaches, namely, SD-OCT, to understand the pathogenesis of contact lens–associated fungal keratitis that may be translated into better clinical management of this serious sight-threatening infection.

METHODS

Contact lenses: To develop a good fitting contact lens (CL) rat model, we performed in vivo OCT imaging of the rat cornea (n=6) and determined the following measurements: corneal radius=3.05 mm (SD=0.07), corneal limbus-to-limbus diameter=5.55 mm (SD=0.08), and eye diameter=6.60 mm (SD=0.15). Hydrogel contact lenses (38% water and 62% polymacon) with the specifications base curve=3.1 mm, diameter=6.0 mm, and thickness=80 µm were designed and manufactured specifically for the rat cornea by Bausch & Lomb (Hastings, UK) according to our OCT measurements.

Animals: Adult female Sprague-Dawley rats (Harlan Laboratories, Allen Park, MI), weighing 250–275 g were used and housed under a 12 h:12 h light-dark cycle with access to food and water ad libitum. Animal use strictly followed the guidelines of the Association for Research in Vision and Ophthalmology (ARVO) Statement for the Use of Animals in Ophthalmic and Vision Research.

Fusarium solani suspension: A clinical isolate recovered during the 2005–2006 outbreak from a patient with contact lens–associated *Fusarium solani* keratitis at Bascom Palmer Eye Institute (BPEI; Miami, FL) was used. The *F. solani* isolate was grown as a pure culture on Sabouraud agar plates for 72 h at 35 °C. A suspension was prepared in sterile saline solution. The concentration of the suspension was determined by counting the conidia in a hemocytometer and adjusting to 10^8 conidia/ml. All of the contact lenses in the experimental group were soaked overnight in 10^8 CFU/ml *F. solani* suspension and the control contact lenses in sterile saline (Unisol 4; Alcon, Fort Worth, TX), before they were fitted on the rat eyes.

Differential interference contrast microscopy of contact lens incubated with Fusarium solani: A representative contact lens was incubated in *F. solani* 10^8 CFU/ml for 1 h and then cultured on non-nutrient agar for 48 h. The control contact lens was incubated for 1 h in sterile saline and cultured on non-nutrient agar. Differential interference contrast microscopy was performed using an Olympus IX50 microscope (Olympus Imaging America, Center Valley, PA) to document the presence or absence of fungi on the contact lens.

Fusarium keratitis initiation: The rats (n=24) were immunosuppressed with an intramuscular injection of 20 mg/kg cyclosporine (Sandimmune 50 mg/ml; Novartis, Basel, Switzerland) three times weekly for 2 weeks, starting a week before the infection [20]. One drop of moxifloxacin hydrochloride ophthalmic solution (Vigamox, Alcon Laboratories, Fort Worth, TX) was administered in both eyes every hour for 4 h, before the contact lens was fitted as prophylaxis to prevent bacterial growth. Based on our pilot studies, bacterial growth impedes the growth of the fungus. Stromal scraping (n=24) was performed with an epithelial scrape in the central 3 mm of the cornea, followed by 4 vertical and 4 horizontal incisions in the stroma using a Beaver 64 blade. The fungal infection was initiated in the left eye by fitting contact lenses soaked overnight in 10^8 CFU/ml *F. solani* suspension for 4 h. The length of time required to induce the infection in our model was suggested by prior pilot studies in which rats were fitted with *F. solani*–infected contact lenses for 4 h (n=3) and overnight (n=3). The rate of infection in both groups was 100%, suggesting that 4 h exposure was sufficient to induce the infection. Three experiments were performed. In each experiment, the rats (n=8) were divided in the two groups, an experimental group (n=6) fitted with contact lenses soaked in fungal suspension and a second control group (n=2) with contact lenses soaked in sterile saline. The number of control animals was smaller because of the limited availability of the contact lenses. The contralateral eye served as an additional control. The contact lenses were removed after 4 h wear, and the rats were monitored daily for signs of infection for a week. Seven days after the contact lens fit and *F. solani* infection, the animals were euthanized, the eyes were removed, and the

corneas were excised immediately. Animals were euthanized by 100% CO_2 inhalation in a chamber provided by Division of Veterinary Medicine at University of Miami, backed-up by cervical dislocation. One half of each cornea was processed for histology, while the other half was homogenized in PBS (137 mM NaCl; 2.7 mM KCl; 10 mM Na_2HPO_4; 2 mM KH_2PO_4; pH=7.4) and used to count the viable fungi in the infected eyes and perform PCR.

The fungal infection in the rat eye was confirmed with several methods: slit-lamp examination and SD-OCT imaging pre- and 7 days post-infection, histopathological analysis and quantitation of the viable fungi in the excised rat corneas, and PCR with specific primers for *F. solani* in corneal homogenates at the end of the experiment, 7 days post-infection.

Slit-lamp examination: Rats were clinically examined with a slit-lamp biomicroscope (Topcon, Oakland, NJ) at baseline, before the contact lens were fitted, day 0, followed by examinations at days 3 and 7. To document the infection, slit-lamp images were acquired at days 0 and 7 post-infection with a Sony DSLR D90 camera (Sony Corporation, Tokyo, Japan).

Spectral domain optical coherence tomography imaging: SD-OCT was performed in the control and experimental infected rats with *F. solani* with the Bioptigen imaging system (Research Triangle Park, NC) at a wavelength of 840 nm at days 0 and 7 post-infection. The Bioptigen system is equipped with an animal management system consisting of a mounting tube and a six-axis platform to allow for rat imaging. SD-OCT images were acquired with an axial resolution of 3 µm. The scan rate was 20,000 A-scans/sec with 1,024 pixels per A-scan. We acquired raster scans consisting of 100 B-scans. Each B-scan has a density of 1,000 A-lines.

Quantitation of viable fungi per cornea: One half of the rat cornea was cut into small pieces and homogenized in 100 µl sterile PBS using a handheld homogenizer (VWR International, Radnor, PA). Ten µl corneal homogenates were plated onto Sabouraud Dextrose agar plates with chloramphenicol and gentamicin (Remel, Lenexa, KS). The plates were incubated at 37 °C, and the number of viable fungi was determined with direct counting after 6 days.

Polymerase chain reaction: Total DNA was extracted from corneal homogenates using DNeasy kit for DNA purification (Qiagen, Valencia, CA) following the manufacturer's protocol. The PCR reactions were performed on a Biometra T-Gradient PCR machine (Gottingen, Germany). The thermal cycling parameters are as follows: 1 cycle at 95 °C for 15 min, followed by 44 cycles with a denaturation step at 95 °C for 30 s, an annealing step at 50 °C for 1 min, and an extension step at 72 °C for 1 min, followed by 1 cycle of extension at 72 °C for 9 min. A negative control was included in all experiments. The amplified products were detected with electrophoresis of an aliquot of 10 µl of each amplicon in a 1.5% agarose gel with ethidium bromide 0.02% in 1X Tris-Acetate-EDTA (TAE) buffer. The DNA bands were visualized under UV illumination (Bio-Rad Universal Hood II, Hercules, CA). A 100 kb molecular weight ladder was included in each run (Invitrogen, Carlsbad, CA). The primer sequences are as follows: ITS5 forward: 5′-GGA AGT AAA AGT CGT AAC AAG G-3′; 5.8S reverse: 5′-AGC CAA GAG ATC CGT TGT TGA-3′ (Invitrogen, Carlsbad, CA).

Histology: For histology, the other half of the rat corneas were fixed in 10% paraformaldehyde and processed for paraffin embedding. Longitudinal corneal sections (8 µm) were processed in the BPEI Histology Core Laboratory with hematoxylin and eosin (H&E), Gomori methenamine silver (GMS), and periodic acid Schiff (PAS) staining according to published protocols. Sections were counterstained with light green for GMS and Mayer's hematoxylin for PAS [21].

Statistical analysis: Values are reported as mean plus standard deviation (SD). The unpaired Student *t* test was used for statistical analyses.

RESULTS

The rat contact lens model development: Custom-made contact lenses were developed based on OCT measurements of the rat corneas. These contact lenses fitted perfectly on the rat eyes. A representative slit-lamp picture and SD-OCT image of the rat eye with the contact lens in place are shown in Figure 1A,B, respectively. Ninety-two percent of the rats maintained the contact lenses for 4 h without any anesthesia or other methods to keep the contact lens in place, such as tarsorrhaphy (Abou Shousha M et al., unpublished results).

Contact lens-associated Fusarium keratitis in the rat: To determine if the *F. solani* isolate forms biofilm on the hydrogel contact lenses, they were incubated with 10^6 CFU/ml *F. solani* for 1 h and then cultured on non-nutrient agar for 48 h. Differential interference contrast microscopy of the contact lenses incubated with *F. solani* revealed biofilm formation with both spores and hyphae (Figure 2A). The presence of spores showed that the fungus was active and producing. The control contact lens was incubated for 1 h in sterile saline and cultured on non-nutrient agar. The contact lens showed no evidence of growth after 48 h (Figure 2B).

To induce *Fusarium* keratitis, a corneal stromal abrasion was performed in the experimental eye, and then the rats were fitted for 4 h with contact lenses contaminated with *F. solani*. Twenty-two out of 24 rats maintained the contact lenses

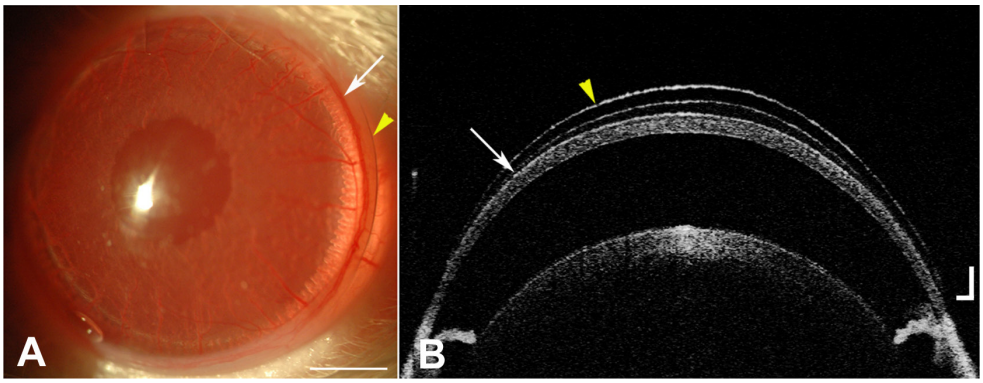

Figure 1. The custom made contact lenses fitted perfectly on the rat eye. **A**: A representative slit-lamp picture illustrates the rat eye with the contact lens in place. The yellow arrowhead points to the margin of the contact lens and the white arrow to the limbus. **B**: The corresponding optical coherence tomography image shows the rat eye with the contact lens in place. The yellow arrowhead points to the contact lens and the white arrow to the cornea. Scale bar=100 µm.

continuously for 4 h, while two were retrofitted, demonstrating that the contact lens model is highly reproducible. The incidence of contact lens–related *Fusarium* keratitis in rats with stromal scraping was 100%.

Slit-lamp examination of the rat eye: Diagnosis and evaluation in microbial keratitis are usually based on slit-lamp examination. Slit-lamp examination of *Fusarium*-infected and control animals established that the onset of opacity appeared 3 days after the infection. After 1 week of infection, we observed severe corneal opacity. Most of the corneas showed abscess formation as shown in Figure 3B. In contrast, slit-lamp examination of the control eyes, fitted with a contact lens soaked in sterile saline, showed no inflammation and was clear (Figure 3A), similar to the eye not fitted with the contact lens.

Spectral-domain optical coherence tomography imaging of the rat cornea: We performed SD-OCT imaging in the *F. solani*–infected and control rats before infection and 7 days post-infection. In vivo SD-OCT detected specific pathological changes in the corneas in fungal keratitis. Figure 3E presents the corresponding SD-OCT image of the infected eye examined with the slit-lamp in Figure 3B. With high correlation, the SD-OCT image shows that the abscess in Figure 3B is hyper-reflective, casting a shadow over the underlying tissue. The tissue planes were unidentifiable, and the anterior surface was irregular. Hyper-reflective plaques over the endothelial side of the cornea were also noted (Figure 3E, arrow). These plaque-like-precipitates are formed of inflammatory cells with or without the causative fungus and commonly seen in fungal keratitis [22]. Infection was confirmed with H&E staining of corneal sections from the same animal 7 days post-infection, showing severe disruption of the tissue architecture, increased corneal thickness, and the presence of endothelial plaques (arrow; Figure 4D,E). The SD-OCT image of the control eye showed normal thickness of the cornea, clear tissue planes, and an intact epithelium. The eyes maintained the normal architecture of the cornea, preserving the endothelium, stroma, and epithelium (Figure 3D), as confirmed with H&E of the normal eye (Figure 4A,B).

Most interestingly, in three cases, only subtle changes in the slit-lamp examination were noted 1 week post-infection

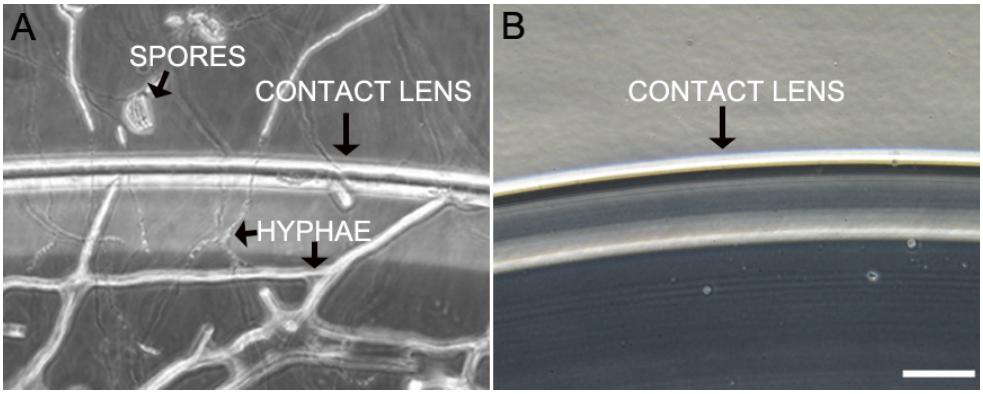

Figure 2. Incubation of contact lenses in *Fusarium solani* suspension resulted in biofilm formation. **A**: Differential interference contrast microscopy shows a representative contact lens soaked in 10^6 CFU/ml *Fusarium solani* suspension and cultured on non-nutrient agar invaded by hyphae and spores. **B**: A control contact lens incubated in sterile saline solution had no growth. Scale bar=100 µm.

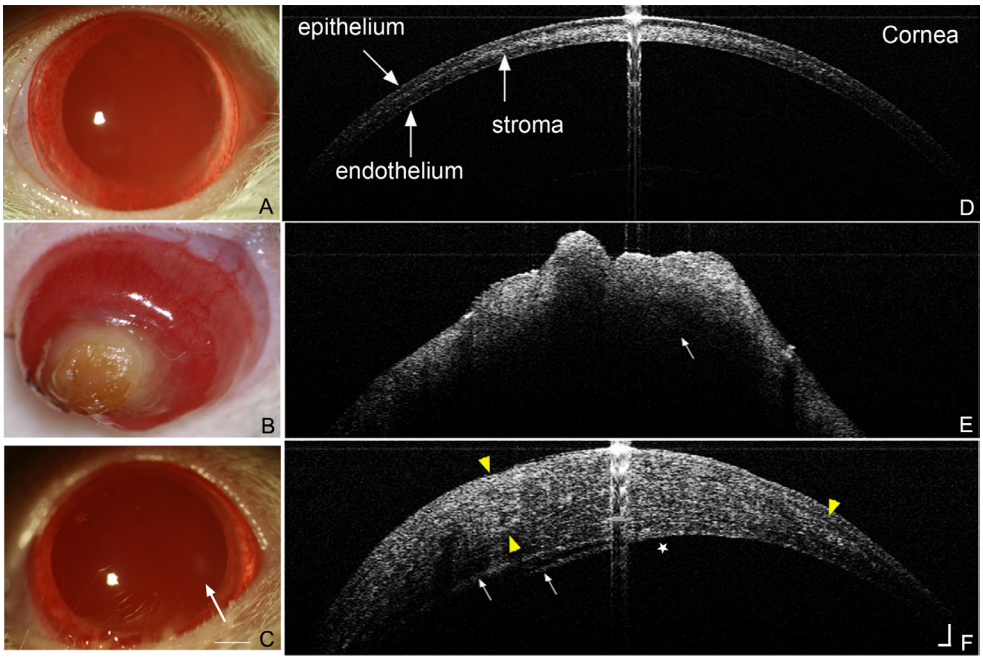

Figure 3. Comparison of slit-lamp pictures to spectral domain optical coherence tomography (SD-OCT) images from representative animals 7 days after contact lens fitting. **A**: Slit-lamp examination of the control eye showed no signs of inflammation. **D**: The corresponding SD-OCT image of the control eye showed normal thickness of the cornea and clear tissue planes. White arrows point to the epithelium, stroma, and endothelium. **B**: Slit-lamp pictures of the eyes fitted with *Fusarium*-soaked contact lenses revealed for the majority of rats severe keratitis with abscess formation. **E**: Corresponding SD-OCT images disclosed an abnormally thickened, hyper-reflective corneal tissue, most likely representing the corneal abscess. Note the absence of the overlying epithelium, unidentifiable tissue planes, and the presence of endothelial plaques (arrow). **C**: In a few cases the slit-lamp picture of the rat eye showed only subtle infiltrates (white arrow). **F**: In contrast, the SD-OCT image of the same eyes showed increased corneal thickening, several areas of hyper-reflectivity representing infiltrates (yellow arrowheads), and endothelial plaques (white arrows). Stromal edema resulted in a change in the convexity of the posterior corneal surface (white star). Scale bar=100 µm.

(Figure 3C). In these cases, slit-lamp diffuse illumination showed only subtle stromal haze, while the slit-lamp optical section showed areas of thickening and subtle haze in the stroma that likely represented infiltrates (Figure 3C, arrow). In contrast to the slit-lamp examination, SD-OCT imaging of the same eye (Figure 3F) showed definite pathological features such as increased corneal thickening, non-identifiable tissue planes, loss of epithelial continuity, with an irregular raised epithelial surface, and several hyper-reflective areas that were most probably infiltrates (yellow arrowheads). Stromal edema resulted in a change in the convexity of the posterior corneal surface (star), and there were clear inflammatory plaques characteristic of the fungal infection (arrow). Histology of this infected eye confirmed with high-correlation moderate keratitis with focal infiltrates (Figure 4G,H, yellow arrowheads) and endothelial plaques (Figure 4G, arrows).

Histopathology of rat Fusarium keratitis: Seven days post-infection, after slit-lamp and SD-OCT imaging, at the end of experiment the animals were euthanized, and their corneas were processed for histology. To confirm the fungal infection, we performed more specific fungal stains such as GMS and PAS, which stain most fungi, viable or dead.

The H&E staining showed disruption of the tissue architecture of the cornea in the *Fusarium*-infected eyes, compared with control, non-infected eyes. Most of the *Fusarium*-infected animals 7 days post-infection manifested severe keratitis with increased corneal thickness, endothelial plaques (Figure 4D, black arrow), and severe inflammation with many infiltrating polymorphonuclear neutrophils (PMNs), significant necrosis, and fibrosis (Figure 4E). A marked number of fungal filaments had invaded every layer of the cornea up to the stroma as identified with GMS (Figure 4F, red arrows) and PAS (data not shown). In contrast, the control eye fitted with a contact lens soaked in PBS exhibited normal corneal architecture (Figure 4A,B), and GMS staining showed no fungal elements (Figure 4C). Histopathological analysis of the representative *Fusarium*-infected eye imaged in Figure 3C,F revealed mild to moderate keratitis with increased corneal thickness, edema, endothelial plaques (arrows), and mostly focal inflammation (yellow arrowheads) with a moderate number of PMNs (Figure 4G,H). A small number of fungal hyphae in the corneal stroma was identified with GMS staining (Figure 4I, red arrows).

Quantitation of viable fungi per cornea: Typical *F. solani* growth was noted on the culture plates of the infected eyes

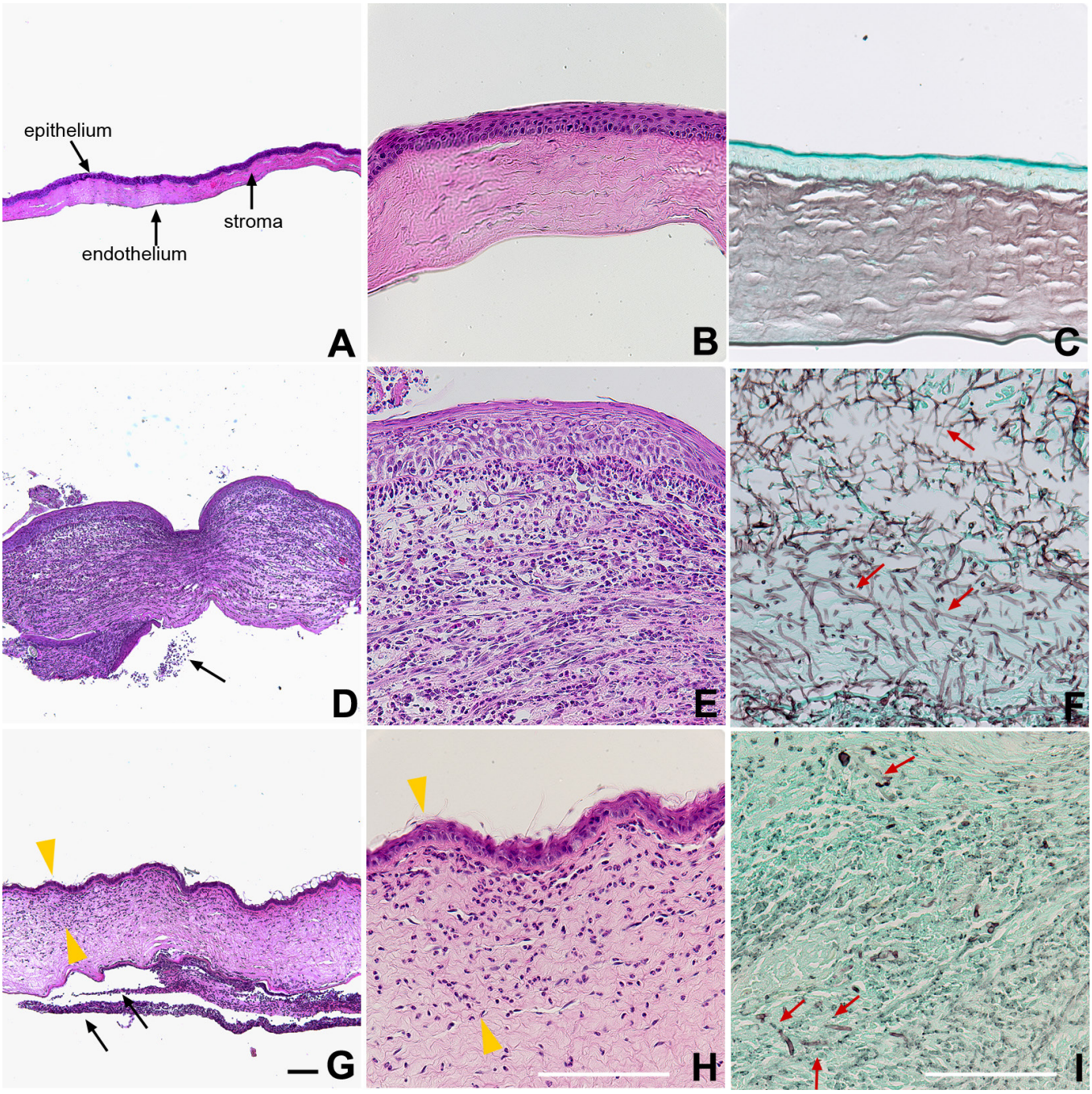

Figure 4. Histopathological analysis of rat *Fusarium* keratitis. **A**–**C** illustrate histology of a corneal button from a representative control rat fitted with a contact lens soaked in saline. **A**, **B**: Hematoxylin and eosin (H&E) staining showed normal corneal caliber and absence of inflammatory infiltrates. **C**: Gomori methenamine silver (GMS) staining showed no fungal elements. **D**–**F** show a corneal button from a representative rat fitted with a contact lens soaked in *Fusarium solani* suspension with severe keratitis. **D**, **E**: H&E staining showed increased corneal thickness, severe inflammation, and necrotic stroma. **F**: A marked amount of fungal elements consistent with *Fusarium* were identified by GMS (red arrows). **G**–**I** illustrate a corneal button from a rat fitted with a contact lens soaked in *Fusarium* solution with mild to moderate keratitis. **G**, **H**: H&E staining showed increased corneal thickness, edema, and a moderate amount of polymorphonuclear neutrophils (yellow arrows). **I**: A mild amount of fungal hyphae in the corneal stroma was identified with GMS (red arrows). **D**, **G**: Note the presence of endothelial plaques (black arrows). Scale bar=100 µm.

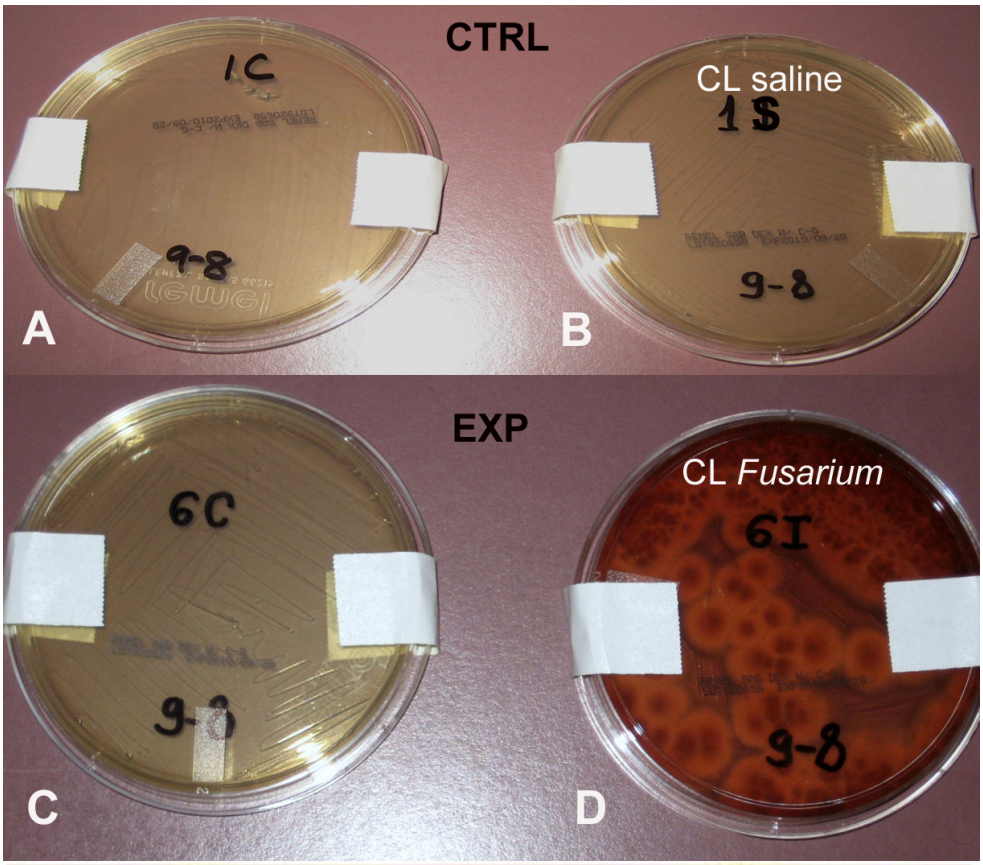

Figure 5. Corneas from rats fitted with contact lenses soaked in *Fusarium* suspension showed typical *Fusarium solani* growth when cultured on Sabouraud agar plates. One week post-infection corneas from rats fitted with contact lenses soaked in control saline, and *Fusarium* suspension were removed, homogenized, and cultured on Sabouraud agar plates for 6 days. **A**, **B**: Both corneas of a representative control animal (CTRL), one from the eye fitted with a contact lens soaked in sterile saline (CL saline), and the other from the contra-lateral eye, not fitted with a contact lens, showed no microbial growth. **C**, **D**: The cornea from a representative experimental animal (EXP) fitted with a *Fusarium* infected contact lens (CL *Fusarium*) showed typical *Fusarium solani* growth, while the contra-lateral eye showed no growth.

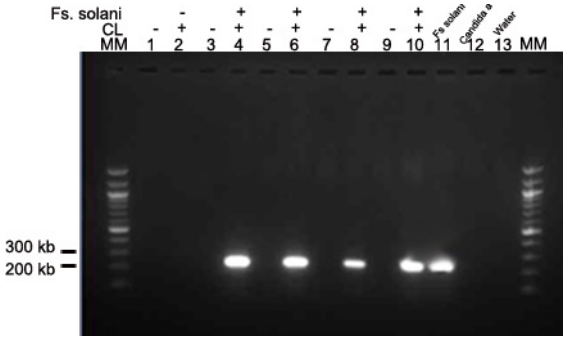

Figure 6. All the rats showing signs of fungal keratitis were PCR positive with primers specific for *Fusarium*. Agarose gel of PCR products from representative rats fitted with contact lenses (CL; +), while the contra-lateral eye served as a control (-). The contact lenses were soaked overnight in *Fusarium solani* (+) for experimental rats or PBS (-) for controls, before fitting on the rat eye. The presence of a 250–300 bp band characteristic of *Fusarium sp.* was detected only in the lanes (4, 6, 8, 10) corresponding to the eyes fitted with *Fusarium*-soaked contact lenses. Lane 2 corresponds to control eye fitted with a contact lens soaked in saline solution, while lanes 1, 3, 5, 7, 9 represent contra-lateral eyes not fitted with contact lenses. Both types of control eyes were negative. DNA from an ATCL *F. solani* strain was used as positive control (lane 11). Candida albicans and water were used as negative controls (lanes 12, 13). MM=λ ladder molecular marker.

(Figure 5D). The control eyes did not show viable fungi (Figure 5B). Six days post-plating, direct plate counting was performed to quantify the viable fungi. We obtained 10^5 CFU/eye, which reflects a good recovered infective dose.

Polymerase chain reaction diagnosis of Fusarium keratitis in the contact lens rat model: We next tested corneal homogenates from experimental and control rats with PCR to identify the presence of *Fusarium*. All rats showing signs of infection were PCR positive with primers specific for *Fusarium sp.* A band of 250–300 bp characteristic of *Fusarium sp.* appeared only in the lanes corresponding to the infected eyes (Figure 6). This is in agreement with previous

studies that used PCR to diagnose *Fusarium* keratitis in rabbits and had an 89% identification rate [23].

DISCUSSION

In this study, we developed a highly reproducible rat contact lens model. Custom-made contact lenses that fit the rat eyes perfectly were constructed based on specifications determined with in vivo OCT measurements of the rat eyes. Using custom-made contact lenses in our experiments enabled the rats to maintain the lenses for at least 4 h without any anesthesia or other methods to keep the contact lens in place such as tarsorrhaphy, mimicking overnight and extended contact lens wear in humans.

As the first approach testing this new contact lens model, we induced and characterized *Fusarium* keratitis, due to its importance and morbidity. Other studies have reported successful rodent models of contact lens–associated *Fusarium* keratitis [24]. However, in those studies mice were fitted with human contact lenses punched to fit the mouse eye, and the mice were reported to be anesthetized to keep the contact lens in place during the 2 h initiation of infection time. Our new contact lens rat model is a valuable tool that can be used in the future to study contact lens–related complications, such as other types of microbial keratitis and contact lens–related chronic inflammation. This model represents an excellent preclinical platform for evaluating new therapies. The clinical presentation in the rat contact lens–related *Fusarium* keratitis model evaluated with slit-lamp examination, correlated with SD-OCT, PCR, culture, and histopathology results and showed that we successfully induced contact lens *Fusarium* keratitis in the rat, which is similar to the human disease.

Earlier studies showed that fungal isolates do not bind to intact corneal epithelium, but adhere to the stroma, denuded of the epithelium [25]. More recently, Sun Y et al. demonstrated that fitting mice with intact, un-scraped corneas with *Fusarium*–infected contact lenses does not induce keratitis, indicating that the intact corneal epithelium is an effective barrier to infection, and fungi cannot penetrate it [24]. Fungi can gain access into the cornea only through a defect in the epithelium resulting from trauma primarily during agricultural work [22], or associated with prior corneal surgery, or contact lens wear. Studies have shown that contact lenses cause a breach in the local protective mechanisms of the eye and can cause impaired corneal metabolism and integrity, decreased epithelial thickness and metabolic rate, lactate accumulation, increased endothelial polymegathism, stromal thinning, limbal redness, and vascularization. These corneal changes have been correlated with contact lens wear complications, including keratitis [26,27]. To mimic these contact lens–induced changes, we performed stromal scraping on rat eyes before fitting them with *Fusarium*-soaked contact lenses and obtained a 100% rate of infection. This suggests that the fungal infection might require more than a superficial scratch on the cornea to develop and that the cells and their receptors responsible for initially recognizing *Fusarium* conidia are localized deeper in the stroma. Indeed, a role for stromal macrophages in mediating *Fusarium* and *Candida* keratitis was identified [28]. In a recent study, Leal et al. injected labeled red fluorescent protein (RFP) *Aspergillus fumigatus* conidia into the stroma of Mafia mice, in which green fluorescent protein (GFP)-labeled macrophages and dendritic cells can be depleted, and showed that resident stromal macrophages and dendritic cells expressing Dectin-1 receptors, rather than the corneal epithelial or fibroblast cells, are essential for fungal recognition and killing in the cornea [29]. Dectin-1 is the receptor for β-glucan, a component of the fungal cell wall exposed when resting fungal conidia reach the stroma and begin germinating and forming hyphae [30]. In good correlation, Dectin-1 is abundantly expressed in stromal macrophages and dendritic cells in corneal samples from patients with *Fusarium* or *Aspergillus* corneal ulcers [31]. These data are consistent with a model in which resting fungal conidia reach the corneal stroma and initiate the infection by germinating and exposing β-glucan, which recognizes and binds to Dectin-1 receptors on the surface of resident macrophages and dendritic cells. This interaction initiates signaling cascades in macrophages that lead to secretion of inflammatory cytokines and recruitment of PMNs to the corneal stroma, which in turn causes corneal opacification but eventually results in fungal killing and tissue healing with scar formation. However, impairment of tissue response at any stage would lead to uncontrolled fungal growth and result in corneal perforation.

One of the key elements for successfully treating fungal keratitis is early diagnosis. In fungal keratitis, diagnosis is based on slit-lamp examination of clinical features of corneal epithelial defect and stromal infiltrate and identifying the pathogen primarily with microscopic examination and fungal culture but also with newer methods such as PCR and/or confocal microscopy [23,32-36]. Current treatment methods require prolonged therapy with antifungal agents, and frequently fail to preserve or restore vision after fungal keratitis. Disease progression and response to treatment are also assessed with slit-lamp examination. However, slit-lamp examination has limited magnification and cannot accurately determine the depth and the extent of the pathological features of the infection [18]. In the present study, we used novel, non-contact SD-OCT imaging technology to evaluate the rat cornea after contact lens–related *Fusarium solani* infection.

We showed that SD-OCT images correlate well with slit-lamp examination, but even better with histopathological analysis. At the slit-lamp, infected corneas presented with edema and dense infiltrates, which were seen on the SD-OCT as areas of hyper-reflectivity and stromal thickening. The high-resolution of the SD-OCT images revealed additional pathological features such as loss of physiologic demarcation between corneal layers, changes in the convexity of the cornea surface, and endothelial plaques. We defined SD-OCT signs of infection, namely, the accurate detection of areas of infiltration, which appeared as hyper-reflective and thickened tissue, as well as visualization of endothelial changes, such as endothelial plaques. Interestingly, in three rats that received *Fusarium*-infected contact lenses the signs of the disease obtained with slit-lamp examination, using diffuse and optical section illumination, were subtle. Surprisingly, SD-OCT of the cornea disclosed significant signs of infection by demonstrating corneal thickening and infiltration, in addition to endothelial plaques. In the most sophisticated clinics, patients are evaluated with SD-OCT only when they are symptomatic enough; therefore, it is difficult to determine the early changes in keratitis. This emphasizes the use of our contact lens wear animal model that identifies early changes and may assist in early diagnosis of the disease.

In the future, we plan to evaluate the imaging features of the cornea with SD-OCT as a function of disease progression, to provide a natural history of *Fusarium* keratitis. In addition, future studies will assess quantitative changes in the corneal thickness and infiltrate. Using our model will allow the study of the progression of the infection and response to treatment at the molecular and cellular levels and identification of specific optical signs on SD-OCT that can be translated into clinical studies on human subjects. In addition, exploring whether the SD-OCT signs of infection are typical of fungal keratitis requires a method for differentiating between fungal and bacterial keratitis. Future studies are necessary to assess the role of OCT in diagnosing other types of keratitis such as *Acanthamoeba* keratitis.

In summary, in this study we demonstrated a highly reproducible rat contact lens model with the help of OCT. We successfully induced *Fusarium* keratitis in the animal model. We used the model to demonstrate the potential role of SD-OCT in evaluating fungal infection and showed that SD-OCT could help to detect subclinical infection. This model has great potential to help us evaluate the molecular, cellular, and imaging features of infectious keratitis development.

ACKNOWLEDGMENTS:

The authors would like to thank Joe Barr, OD, MS and Eoin O'Dunlaing, charter engineer at Bausch & Lomb for their valuable help in developing custom made contact lenses for rats and Eleut Hernandez at Bascom Palmer Eye Institute for his help with the animal studies. Supported in part by Allergan Horizon Fellowship Grant (MAS), University of Miami Scientific Awards Committee Pilot Grant (MLB). The Bascom Palmer Eye Institute is supported by a National Institutes of Health Core Grant NIHP301430 and an unrestricted grant from Research to Prevent Blindness.

REFERENCES

1. Thylefors B, Negrel AD, Pararajasegaram R, Dadzie KY. Available data on blindness (update 1994). Ophthalmic Epidemiol 1995; 2:5-39. [PMID: 7585234].
2. Dart JK, Radford CF, Minassian D, Verma S, Stapleton F. Risk factors for microbial keratitis with contemporary contact lenses: a case-control study. Ophthalmology 2008; 115:1647-54. [PMID: 18597850].
3. Green M, Apel A, Stapleton F. Risk factors and causative organisms in microbial keratitis. Cornea 2008; 27:22-7. [PMID: 18245962].
4. Liesegang TJ, Forster RK. Spectrum of microbial keratitis in South Florida. Am J Ophthalmol 1980; 90:38-47. [PMID: 7395957].
5. Wong TY, Ng TP, Fong KS, Tan DT. Risk factors and clinical outcomes between fungal and bacterial keratitis: a comparative study. CLAO J 1997; 23:275-81. [PMID: 9348453].
6. Keay LJ, Gower EW, Iovieno A, Oechsler RA, Alfonso EC, Matoba A, Colby K, Tuli SS, Hammersmith K, Cavanagh D, Lee SM, Irvine J, Stulting RD, Mauger TF, Schein OD. Clinical and microbiological characteristics of fungal keratitis in the United States, 2001–2007: a multicenter study. Ophthalmology 2011; 118:920-6. [PMID: 21295857].
7. Center for Disease Control and Prevention2006
8. Alfonso EC, Miller D, Cantu-Dibildox J, O'Brien TP, Schein OD. Fungal keratitis associated with non-therapeutic soft contact lenses. Am J Ophthalmol 2006; 142:154-5. [PMID: 16815266].
9. Cohen EJ. Fusarium keratitis associated with soft contact lens wear. Arch Ophthalmol 2006; 124:1183-4. [PMID: 16908822].
10. Gower EW, Keay LJ, Oechsler RA, Iovieno A, Alfonso EC, Jones DB, Colby K, Tuli SS, Patel SR, Lee SM, Irvine J, Stulting RD, Mauger TF, Schein OD. Trends in fungal keratitis in the United States, 2001 to 2007. Ophthalmology 2010; 117:2263-7. [PMID: 20591493].
11. Ma SK, So K, Chung PH, Tsang HF, Chuang SK. A multi-country outbreak of fungal keratitis associated with a brand

of contact lens solution: the Hong Kong experience. Int J Infect Dis 2009; 13:443-8. [PMID: 19019715].

12. Gaujoux T, Chatel MA, Chaumeil C, Laroche L, Borderie VM. Outbreak of contact lens-related *Fusarium* keratitis in France. Cornea 2008; 27:1018-21. [PMID: 18812765].
13. Yehoshua Z, Rosenfeld PJ, Gregori G, Feuer WJ, Falcao M, Lujan BJ, Puliafito C. Progression of geographic atrophy in age-related macular degeneration imaged with spectral domain optical coherence tomography. Ophthalmology 2011; 118:679-86. [PMID: 21035861].
14. Aref AA, Budenz DL. Spectral domain optical coherence tomography in the diagnosis and management of glaucoma. Ophthalmic Surg Lasers Imaging 2010; 41:SupplS15-27. .
15. Shen M, Wang MR, Yuan Y, Chen F, Karp CL, Yoo SH, Wang J. SD-OCT with prolonged scan depth for imaging the anterior segment of the eye. Ophthalmic Surg Lasers Imaging 2010; 41:SupplS65-9. .
16. Shousha MA, Perez VL, Wang J, Ide T, Jiao S, Chen Q, Chang V, Buchser N, Dubovy SR, Feuer W, Yoo SH. Use of ultra-high-resolution optical coherence tomography to detect in vivo characteristics of Descemet's membrane in Fuchs' dystrophy. Ophthalmology 2010; 117:1220-7. [PMID: 20163865].
17. Ide T, Wang J, Tao A, Leng T, Kymionis GD, O'Brien TP, Yoo SH. Intraoperative use of three-dimensional spectral-domain optical coherence tomography. Ophthalmic Surg Lasers Imaging 2010; 41:250-4. [PMID: 20307045].
18. Konstantopoulos A, Kuo J, Anderson D, Hossain P. Assessment of the use of anterior segment optical coherence tomography in microbial keratitis. Am J Ophthalmol 2008; 146:534-42. [PMID: 18602080].
19. Konstantopoulos A, Yadegarfar G, Fievez M, Anderson DF, Hossain P. In vivo quantification of bacterial keratitis with optical coherence tomography. Invest Ophthalmol Vis Sci 2011; 52:1093-7. [PMID: 20926816].
20. Mochizuki M, Nussenblatt RB, Kuwabara T, Gery I. Effects of cyclosporine and other immunosuppressive drugs on experimental autoimmune uveoretinitis in rats. Invest Ophthalmol Vis Sci 1985; 26:226-32. [PMID: 3871750].
21. Prophet EBMB, Arrington JB, Sobin LH. Laboratory Methods in Histotechnology. Washington, DC: Armed Registry of Pathology; 1994.
22. Thomas PA. Fungal infections of the cornea. Eye (Lond) 2003; 17:852-62. [PMID: 14631389].
23. Alexandrakis G, Jalali S, Gloor P. Diagnosis of *Fusarium* keratitis in an animal model using the polymerase chain reaction. Br J Ophthalmol 1998; 82:306-11. [PMID: 9602631].
24. Sun Y, Chandra J, Mukherjee P, Szczotka-Flynn L, Ghannoum MA, Pearlman E. A murine model of contact lens-associated *Fusarium* keratitis. Invest Ophthalmol Vis Sci 2010; 51:1511-6. [PMID: 19875664].
25. Rao NA, Riggio DW, Delmage JM, Calandra AJ, Evans S, Lewis W. Adherence of Candida to corneal surface. Curr Eye Res 1985; 4:851-6. [PMID: 3899521].
26. Efron N. Contact Lens Complications. Oxford: Butterworth-Heinemann; 1999.
27. Ladage PM, Yamamoto K, Ren DH, Li L, Jester JV, Petroll WM, Cavanagh HD. Effects of rigid and soft contact lens daily wear on corneal epithelium, tear lactate dehydrogenase, and bacterial binding to exfoliated epithelial cells. Ophthalmology 2001; 108:1279-88. [PMID: 11425688].
28. Hu J, Wang Y, Xie L. Potential role of macrophages in experimental keratomycosis. Invest Ophthalmol Vis Sci 2009; 50:2087-94. [PMID: 19074808].
29. Leal SM Jr, Cowden S, Hsia YC, Ghannoum MA, Momany M, Pearlman E. Distinct roles for Dectin-1 and TLR4 in the pathogenesis of *Aspergillus fumigatus* keratitis. PLoS Pathog 2010; 6:e1000976-[PMID: 20617171].
30. Gersuk GM, Underhill DM, Zhu L, Marr KA. Dectin-1 and TLRs permit macrophages to distinguish between different *Aspergillus fumigatus* cellular states. J Immunol 2006; 176:3717-24. [PMID: 16517740].
31. Karthikeyan RS, Leal SM Jr, Prajna NV, Dharmalingam K, Geiser DM, Pearlman E, Lalitha P. Expression of innate and adaptive immune mediators in human corneal tissue infected with *Aspergillus* or *Fusarium*. J Infect Dis 2011; 204:942-50. [PMID: 21828275].
32. Srinivasan M. Fungal keratitis. Curr Opin Ophthalmol 2004; 15:321-7. [PMID: 15232472].
33. Miller WL, Giannoni AG, Perrigin J. A case of *Fungal keratitis*: a clinical and in vivo confocal microscopy assessment. Cont Lens Anterior Eye 2008; 31:201-6. [PMID: 18595770].
34. Vaddavalli PK, Garg P, Sharma S, Sangwan VS, Rao GN, Thomas R. Role of confocal microscopy in the diagnosis of fungal and acanthamoeba keratitis. Ophthalmology 2011; 118:29-35. [PMID: 20801515].
35. Vengayil S, Panda A, Satpathy G, Nayak N, Ghose S, Patanaik D, Khokhar S. Polymerase chain reaction-guided diagnosis of mycotic keratitis: a prospective evaluation of its efficacy and limitations. Invest Ophthalmol Vis Sci 2009; 50:152-6. [PMID: 18689703].
36. Oechsler RA, Feilmeier MR, Ledee DR, Miller D, Diaz MR, Fini ME, Fell JW, Alfonso EC. Utility of molecular sequence analysis of the ITS rRNA region for identification of *Fusarium* spp. from ocular sources. Invest Ophthalmol Vis Sci 2009; 50:2230-6. [PMID: 19136697].

Articles are provided courtesy of Emory University and the Zhongshan Ophthalmic Center, Sun Yat-sen University, P.R. China. The print version of this article was created on 27 December 2013. This reflects all typographical corrections and errata to the article through that date. Details of any changes may be found in the online version of the article.